

RED SUPERGIANTS IN M33 GALAXY

O. VASSILEV¹, L. VASSILEVA², G. IVANOV¹ and D. VASSILEV³

(1) Department of Astronomy, University of Sofia, James Bourchier 5, Sofia 1164, Bulgaria

(2) Institute of Astronomy, Bulgarian Academy of Sciences, 72 Tsarigradsko chaussée, BG - 1784 Sofia, Bulgaria

(3) Department of Informatics, Sofia University, James Bourchier Ave. 5, BG - 1164 Sofia, Bulgaria

E-mail ovassilev@tenzor-bg.com

E-mail lubav@astro.bas.bg

E-mail ivanov@phys.uni-sofia.bg

E-mail dvassilev@ucc.uni-sofia.bg

Abstract. In the present work the spatial distribution of the red supergiants in M33 galaxy is discussed. The observational data exhibit stellar groups of high stellar density. The smallest 60 groups with stellar density corresponding to signal-to-noise ratio $S/N > 5$ have a mean size of $8.1''$ (≈ 30 pc). They are real stellar associations in M33. The size of the largest stellar groups found in M33 is of about $200''$ (~ 0.8 kpc) and is typical for a stellar complex.

1. OBSERVATIONAL DATA AND RED SUPERGIANTS SAMPLES

We applied an approach, proposed by Popov et al. (2002), to obtain a continuous picture of the spatial distribution of the brightest stars in M33 galaxy. Their JHK photometry is published in the *Two Micron All Sky Survey* (2MASS). The initial sample of stars was selected using a square field with a width of 1.5° and centered on M33 nucleus (Table 1). Figure 1 illustrates the differences between the stellar populations, occupying areas of equal angular size outside the boundaries of the galaxy (Fig. 1a) and within its effective diameter (Fig. 1b). Several hundreds of stars have been detected (Table 2) at the red end of the evolutionary tracks (Lejeune et al. 1997); they are most probably red supergiants (RSGs) in the mass range of $12-20 M_\odot$. Figure 2 clearly shows the location of the stellar disk cut off along the major axis: $a = 32'$ at ($S/N < 3$). It is natural to set a limit $K > 13^m$ since brighter stars should belong to the Milky Way (Fig. 1) - the total number of objects in the sample with this single restriction (Sample 1) is denoted as N_1 . Another sample is a subsample of Sample 1 and contains stars selected by criterion $J - K > 1.1$ which leads to even stronger S/N ratio and also testifies that the stellar disk ends at $a \approx 30'$ along the major axis (see Fig.3). Further we take into consideration only a sample of

Table 1: General information on M33 galaxy

Center's (nucleus) coordinates (de Vaucouleurs & Leach 1981):

$$\alpha(2000) = 01^{\text{h}}33^{\text{m}}50.89^{\text{s}}$$

$$\delta(2000) = +30^{\circ}39'36.7''$$

Fundamental observables (RC3):

$$D_{25} = 35.4'$$

$$(a/b) = 1.698$$

$$a_{\text{eff}} = 13.5'$$

Positional angle P. A. = 23°

Inclination angle $i = 54.3^{\circ}$

Distance modulus (Lee *et al.* 2002):

$$m - M = 24.52^{\text{m}}$$

Foreground extinction (Schlegel *et al.* 1998):

$$E_{\text{B-V}} = 0.135$$

$$E_{\text{J-K}} = 0.072 ; A_{\text{K}} = 0.050$$

$N_2 = 1650$ stars populating the whole area $1.5^{\circ} \times 1.5^{\circ}$ and constrained by conditions: $K > 13^{\text{m}}$ and $J - K > 1.1$ (Sample 2).

2. SURFACE BRIGHTNESS AND COLOUR MAPS

The individual J and K magnitudes of the stars with rectangular coordinates X and Y, relative to M33 center, represented by δ -functions, were convoluted with 2D gaussians ($\sigma = 50''$), cut-off level at 3σ . Their contribution to the surface brightness in each pixel is calculated by: $\mu = -2.5 \log(10^{-0.4 m} / (\text{pixel size})^2)$. The chosen scale of $5''/\text{pixel}$ gives an image of 1020×1020 pixels after removal of $150''$ strips from both sides in X and Y in order to avoid edge effects. The adopted foreground surface brightnesses μ_1 (Sample 1) and μ_2 (Sample 2) are given in Table 3. For their calculation we used a hexagonal grid consisting of about 200 independent measurements of the foreground surface brightness.

The choice of $\sigma = 50''$ conditioned by our intent to recover the grand design features of M33. We expected to find structures not smaller than $150''$ (~ 0.6 kpc at the distance of M33), i.e. stellar complexes or spiral arms of $1/2$ arm width.

3. THE MAIN RESULTS

1. The spiral pattern of M33 is delineated as area with high density of RSGs (Fig. 3) and with surface brightness μ_2 (in K passband) larger than $23 \text{ mag.arcsec}^{-2}$ (Fig. 4).
2. The spiral structure is patchy - there were detected several regions of enhanced surface brightness, especially in the central region ($15'' \times 15''$). Their size of about $200''$ (~ 0.8 kpc) is typical of a stellar complex (Fig. 4).
3. A pair of dusty arms is visible on ($J-K$) color map (Fig. 5). They surround the central region of maximal K-surface brightness. Assuming the mean $\langle J - K \rangle = 1.2$

to be the true color for a red supergiant and $\langle J - K \rangle = 1.8$ at the ridges of the dusty arms, a value of $A_V = 3$. could be derived which reflects 1/2 of the optical depth of the disk: $1.086 \tau_V = 2 A_V$. A rough estimate of the vertical optical depth in the dusty arms is obtained: $\tau_B = 4.5$, with preliminary correction for inclination (factor $a \cos(i)$) and postulating $A_B = 1.331 A_V$. The disk of M33 seems to be optically thick at least at the ridges of its spiral arms - like in the case of other nearby spiral galaxy M31 (Nedialkov & Ivanov 1999).

4. An impressive coincidence exists between the K-band surface brightness map and the H-alpha emission map (Fig. 6). This indicates that the RSGs and their progenitors OB stars (not visible in IR) are well mixed in the space and the star formation in M33 disk has been a continuous process over the last 10 Myr.

Table 2: Foreground contamination in the field of M33 galaxy derived from counts in elliptical rings of one and the same area of 200 arcmin². The expected number of MW stars is $N_1 = (138 \pm 12)$ for Sample 1, and $N_2 = (15 \pm 4)$ Sample 2.

a'	N_1	cont. %	N_2	cont. %
12.6	819	16.8	431	3.5
16.4	451	30.6	214	7.0
19.4	367	37.6	180	8.3
22.0	309	44.7	118	12.7
24.4	239	57.7	79	19.0
26.5	188	73.4	48	31.3
28.5	177	78.0	48	31.3
30.3	159	86.8	34	44.1
32.0	156	88.5	35	42.9
33.7	130	106.2	16	93.8
35.3	162	85.2	20	75.0
36.8	138	100.0	21	71.4
38.2	140	98.6	13	115.4

Table 3: Adopted foreground surface brightnesses in [mag.arcsec⁻²] in J and K pass-bands: μ_1 for Sample 1 and μ_2 for Sample 2.

Band	μ_1	μ_1 ($S/N = 5$)	μ_2	μ_2 ($S/N = 5$)
J	24.7 ± 0.6	24.0	28.7 ± 1.0	27.5
K	24.0 ± 0.4	23.1	27.3 ± 0.9	26.1

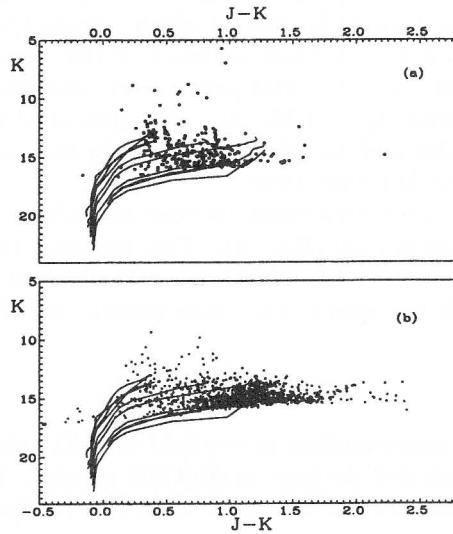


Fig. 1: Colour-magnitude diagrams K vs. $J - K$ for areas of equal angular size in: (a) foreground field, and (b) within the effective diameter of M33. Note the strong crowding of RSGs at $K = 13^m - 16^m$ and $J - K = 1.2^m$. The evolutionary tracks (solid lines) for stars with initial mass between $12-60 M_{\odot}$ are also shown.

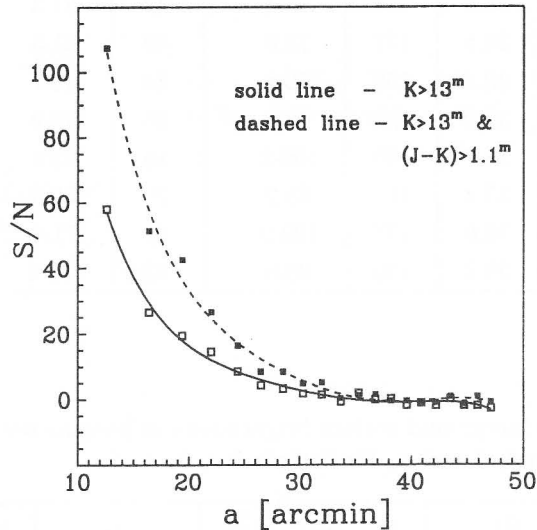


Fig. 2: The signal-to-noise ratio versus major axes of elliptical rings of one and the same area: 200 arcmin^2 .

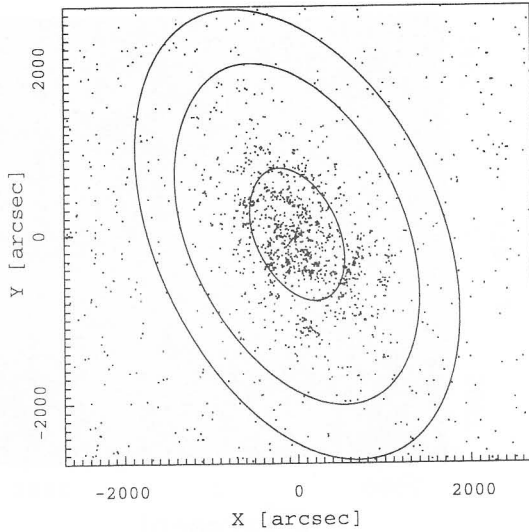


Fig. 3: Program field and spatial distribution of the stars (filled circles) from Sample 2 ($K > 13^m$ and $J - K > 1.1^m$). The size of the smallest ellipse corresponds to the effective diameter along the major axis, that of the intermediate - to D25, and the outermost ellipse encompasses an area, equal to the area outside of it.

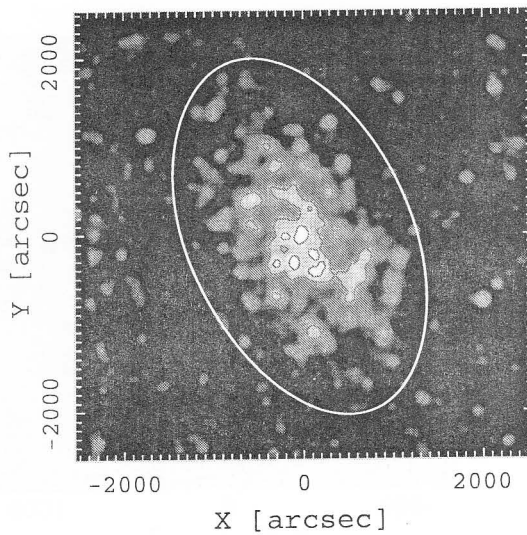


Fig. 4: Gray-scale representation of the surface brightness in K -band. The inner isophote corresponds to $\mu_K = 22 \text{ mag arcsec}^{-2}$ and the outer - to $\mu_K = 24 \text{ mag arcsec}^{-2}$. The gray scale reaches $\mu_K = 24.5 \text{ mag arcsec}^{-2}$ (black). The diameter of the white ellipse is D25'.

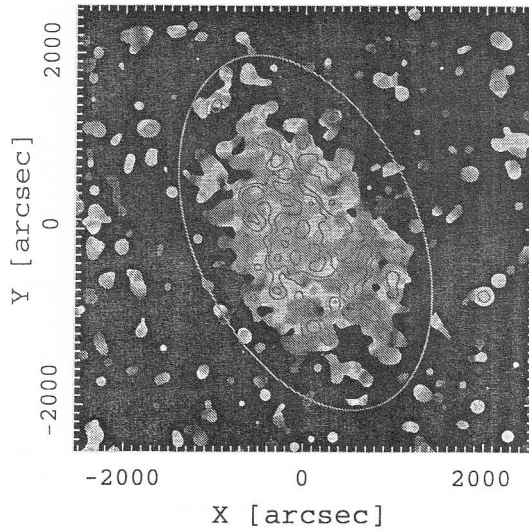


Fig. 5: A false colour map in $(J - K)$ with superimposed isophote $\mu_K = 23 \text{ mag arcsec}^{-2}$. The bluest end is at $(J - K) = 0.8^m$ in violet and the reddest end - at $(J - K) = 2.3^m$ in red. Note the prominent spiral pattern in green ($J - K = 1.8$) indicating the dusty arms.

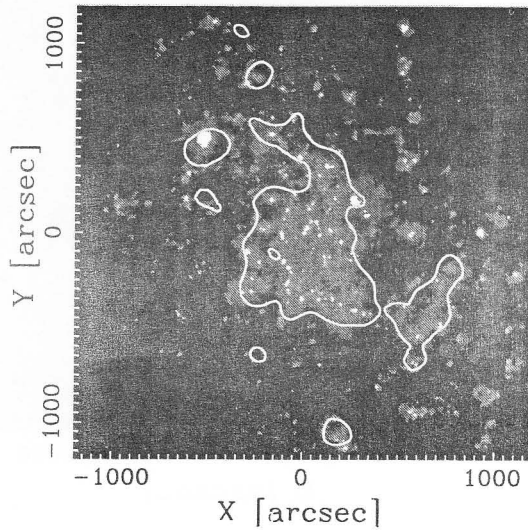


Fig. 6: The surface brightness isophote $\mu_K = 23 \text{ mag arcsec}^{-2}$, superimposed on grey-scale H-alpha map within the inner area $2400'' \times 2400''$ of the program field (Fig. 3).

4. DISCUSSION

In the near future we intend to:

1. Correlate the surface brightness in IR with its estimates in optical passbands and H-alpha.
2. Resolve the stellar associations in M33 via convolution with gaussians of different widths.
3. Study the B/R and WR/R ratio as a function of the galactocentric distance and metallicity and also their variation in the OB associations.
4. Derive precise extinction values from the individual colors of the RSGs.

Acknowledgments

This publication makes use of data from the *Two Micron All Sky Survey*, which is a joint project of the University of Massachusetts and the Infrared Processing and Analysis Center/California Institute of Technology, funded by the National Aeronautics and Space Administration and the National Science Foundation.

O. V. and G. I. acknowledge the partial support by the contract Nr. F-825/1998 with the Bulgarian National Science Foundation, Ministry of Education and Sciences.

References

- de Vaucouleurs, G., Leach, R.: 1981, *Publ. Astron. Soc. Pacific*, **93**, 190.
de Vaucouleurs, G., de Vaucouleurs, A., Corwin, H. Jr., Buta, R., Paturel, G., Fouque, P.: 1991, *Third reference catalog of Bright galaxies (RC3)*, Heidelberg, Springer.
Lee, M., Kim, M., Sarajedini, A., Geisler, D., Gieren, W.: 2002, *Astrophys. J.*, **565**, 959.
Lejeune, T., Cuisinier, F., Buser, R.: 1997, *Astron. Astrophys. Suppl. Series*, **125**, 229.
Nedialkov, P., Ivanov, V.: 1999, *Astron. Astrophys. Trans.*, **17**, 367.
Popov, G., Nedialkov, P., Roussev, I., Veltchev, T.: 2002, (this meeting).
Schlegel, D., Finkbeiner, D., Davis, M.: 1998, *Astrophys. J.*, **500**, 525.